A fully defined and scalable 3D culture system for human pluripotent stem cell expansion and differentiation

Yuguo Lei[a,b,c,d] and David V. Schaffer[a,b,c,d,1]

Departments of [a]Bioengineering and [b]Chemical Engineering, [c]California Institute for Quantitative Biosciences, and [d]Helen Wills Neuroscience Institute, University of California, Berkeley, CA 94720

Human pluripotent stem cells (hPSCs), including human embryonic stem cells and induced pluripotent stem cells, are promising for numerous biomedical applications, such as cell replacement therapies, tissue and whole-organ engineering, and high-throughput pharmacology and toxicology screening. Each of these applications requires large numbers of cells of high quality; however, the scalable expansion and differentiation of hPSCs, especially for clinical utilization, remains a challenge. We report a simple, defined, efficient, scalable, and good manufacturing practice-compatible 3D culture system for hPSC expansion and differentiation. It employs a thermoresponsive hydrogel that combines easy manipulation and completely defined conditions, free of any human- or animal-derived factors, and entailing only recombinant protein factors. Under an optimized protocol, the 3D system enables long-term, serial expansion of multiple hPSCs lines with a high expansion rate (~20-fold per 5-d passage, for a 10^{72}-fold expansion over 280 d), yield (~2.0×10^7 cells per mL of hydrogel), and purity (~95% Oct4+), even with single-cell inoculation, all of which offer considerable advantages relative to current approaches. Moreover, the system enabled 3D directed differentiation of hPSCs into multiple lineages, including dopaminergic neuron progenitors with a yield of ~8×10^7 dopaminergic progenitors per mL of hydrogel and ~80-fold expansion by the end of a 15-d derivation. This versatile system may be useful at numerous scales, from basic biological investigation to clinical development.

Human pluripotent stem cells (hPSCs), including human embryonic stem cells (hESCs) (1) and induced pluripotent stem cells (iPSCs) (2), have the capacities for indefinite in vitro expansion and differentiation into all cell types within adults (3). They therefore represent highly promising cell sources for numerous biomedical applications, such as cell replacement therapies (4, 5), tissue and organ engineering (6), and pharmacology and toxicology screens (7, 8). However, these applications require large numbers of cells of high quality (4, 6–8). For instance, ~10^5 surviving dopaminergic (DA) neurons, ~10^9 cardiomyocytes, or ~10^9 beta cells are likely required to treat a patient with Parkinson disease (PD), myocardial infarction (MI), or type I diabetes, respectively (9). Additionally, far more cells are needed initially because both in vitro cell culture yields and subsequent in vivo survival of transplanted cells are typically very low. As examples of the latter, only ~6% of transplanted dopaminergic neurons or ~1% of injected cardiomyocytes reportedly survive in rodent models several months after transplantation (10, 11). Furthermore, there are large patient populations with degenerative diseases or organ failure (9), including over 1 million people with PD, 1–2.5 million with type I diabetes, and ~8 million with MI in the United States alone (12). Large numbers of cells are also necessary for applications such as tissue engineering, where for example ~10^{10} hepatocytes or cardiomyocytes would be required for an artificial human liver or heart, respectively (6). Additionally, ~10^{10} cells may be needed to screen a million-compound library once (8), and advances in combinatorial chemistry, noncoding RNAs, and investigations of complex signaling and transcriptional

networks have given rise to large libraries that can be screened against many targets (13). Massive numbers of hPSCs may therefore be needed to deliver on the biomedical promise of these stem cells.

In general, hPSCs require key biological signals from their substrate, and from one another (14, 15), that promote cell survival and rapid proliferation and that culture systems must thus provide. Current 2D-based cell culture systems—which suffer from inherent heterogeneity and limited scalability and reproducibility—are emerging as a bottleneck for producing sufficient numbers of high-quality cells for downstream applications (9, 16). An attractive approach for scaling up production is to move cell culture from 2D to 3D (9, 17), and accordingly several 3D suspension systems have been probed for hPSCs production: cell aggregates (18–21), cells on microcarriers (22, 23), and cells in alginate microencapsulates (24) (*SI Appendix*, Table S1). Although these approaches have some attractive aspects, they also highlight significant challenges for 3D hPSC culture (9) (*SI Appendix*, Table S1) including the following: (*i*) the use of components from human or animal tissue (e.g., Matrigel, serum, and/or albumin), which limit reproducibility and/or scalability, pose risks for pathogen and immunogen transfer (18–24), and are thus problematic for good manufacturing practice (GMP) cell production (25); (*ii*) substantial cell agglomeration that can in some cases lead to differentiation and/or death (22, 23); (*iii*) shear forces in agitated cultures that can compromise cell viability (18–23); (*iv*) limited cell expansion rates and cell yields per volume (18–24); and (*v*) unclear potential for long-term serial expansion. As an example, in a recent culture of hPSCs within alginate hydrogel microspheres in mouse embryonic fibroblast conditioned medium, 5% of the encapsulated single hPSCs remained viable after 7 d, and an ~10- to 20-fold expansion to a peak density of 3×10^6 cells per mL occurred after 20 d (24).

Significance

Human pluripotent stem cells can be cultured in vitro and differentiated into presumably all cell types of the human body, and they therefore represent highly promising cell sources for biomedical applications such as cell therapies, tissue engineering, and drug discovery. These applications require large numbers of high-quality cells, and we report an efficient, defined, scalable, and good manufacturing practice-compatible 3D system for the production of human pluripotent stem cells and their progeny. The ease of use and flexible scalability of this system makes it suitable for numerous applications from the laboratory toward the clinic.

To address these challenges, we report an alternative system that expands and differentiates hPSCs within a thermoreversible hydrogel, composed of a polymeric solution that is liquid at low temperature but solidifies into an elastic hydrogel when warmed. Cells can thus be mixed with the liquid at low temperature, suspended and grown in a solid gel at 37 °C, and harvested and passaged by reliquifying the gel at low temperature. The resulting hydrogel offers many features that benefit hPSC biology and culture, including a 3D environment for rapid cell growth, prevention of large cell aggregate formation, isolation of cells from shear forces, and sufficient porosity for nutrient diffusion. Although thermoreversible materials have been used for culturing primary cells in the laboratory (26), large-scale hPSC culture presents numerous additional challenges and constraints, including apoptosis upon cell dissociation (14) and passaging; low survival, limited proliferation, and loss of pluripotency in suboptimal culture conditions; and a strong preference for defined medium to support downstream biomedical applications. We have accordingly investigated these challenges and developed a chemically defined system with no matrix proteins that is capable of 10^{72}-fold expansion over 60 passages with strong maintenance of pluripotency.

Results

Several hydrogel materials—such as alginate (24, 27), agarose (28), and hyaluronic acid (29)—have been previously investigated for hPSC expansion or differentiation. However, to date thermoreversible materials have not been studied in hPSC culture, despite the fact that they offer a number of promising features for GMP-compatible, large-scale culture. In particular, they are synthetic and defined, biocompatible, and enable cell harvest or passaging by simply changing temperature at the range from 4 °C to 37 °C, a mild process for cells. Also, they can be readily processed (e.g., .into spheres or fibers) for large bioreactors. After initial assessment of several synthesized or commercial available thermoreversible hydrogels, we found single hPSCs could survive and retain pluripotency marker expression in 8–10% (wt/vol) poly(N-isopropylacrylamide)-co-poly(ethylene glycol) (PNIPAAm-PEG) hydrogel (Mebiol Gel) (*SI Appendix*, Fig. S1).

Preliminary investigation showed that cell behavior in this material was significantly affected by multiple factors, including the addition of an inhibitor for the RhoA GTPase signaling effector Rho kinase (ROCK) (30), extent of cell dissociation, the culture medium (3), and initial seeding density. We therefore conducted a multifactorial analysis to assess the promise of this material relative to other materials or to cell-only suspensions, identify the optimal conditions under which it supports the biology and culture of hPSC, and study the potential interactions among numerous parameters. Thirty-six combinations of various factors, including seeding with single cells or clusters; use of ROCK inhibitor (RI); cell seeding density; culture medium; and with or without PNIPAAm-PEG hydrogel scaffold, were tested (Figs. 1 and 2). Specifically, cell dissociation promotes hPSC apoptosis via Rho GTPase signaling (14, 31, 32); however, single-cell seeding enables more reproducible expansion during large-scale hPSC production. hPSCs were thus dissociated into single cells and either directly encapsulated into the hydrogel (termed single-cell seeding) or—based on the poor viability observed for single-cell dissociation in 2D (30)—first cultured in suspension overnight to form small clusters that were subsequently encapsulated in the gel (termed precluster seeding) (Fig. 1A). Also, addition of RI for the first 24 h has been shown to support growth of single hPSCs in liquid suspension culture (19), and we included RI for the whole culture period (4-d RI) to assess its effects on cell expansion. Additionally, low seeding density (∼1–2.5 × 10^5 cells/mL) is often used (*SI Appendix*, Table S1), and we also included medium and high seeding densities (1.0 × 10^6 and 2.5 × 10^6 cells/mL, respectively). Furthermore, two media were

used [mTeSR and completely defined Essential 8 (E8)]. Moreover, hPSC suspension in static liquid medium was also included for comparison with the hydrogel. Finally, iPS–mesenchymal stem cells (MSCs), an iPSC derived from human MSCs (33), were used in this optimization.

The study revealed that (*i*) the hydrogel promoted high expansion rates and prevented cell agglomeration (Figs. 1B and 2A). Culturing single hPSCs in 10% (wt/vol) PNIPAAm-PEG with E8 in the presence of RI led to the formation of dense, uniform, and small spheroids with ∼8-, 10-, or 4.4-fold expansion over 4 d at low, medium, or high seeding density, respectively. However, adding RI for 1 d was insufficient to support single cells (Figs. 1B and 2A). When using mTeSR rather than E8, only moderate (<1.6-fold) or no expansion was reached with 4-d or 1-d RI, respectively, for all of the seeding densities, indicating a negative interaction between mTeSR and the hydrogel scaffold (Figs. 1B and 2A). (*ii*) In the hydrogel and E8, preclustered hPSCs behaved similarly to single hPSCs. However, in the hydrogel and mTeSR with 4-d RI, preclustered hPSCs displayed significantly higher expansion (∼4.5-, 4.5-, 2.1-fold for low, medium, high density, respectively) than single hPSCs (Figs. 1B and 2B), indicating that mTeSR stresses single cells. (*iii*) For all static-suspension cultures in liquid medium without hydrogel, large cell aggregates were found, and only ∼2.8-, 1.6-, or 0.2-fold expansion was achieved for low, medium, or high seeding density, respectively (Figs. 1B and 2C). Agglomeration and low expansion (<2.0-fold) were also found in a large dynamic suspension culture (a spinner flask) without hydrogel scaffold (*SI Appendix*, Fig. S2). No significant difference was found between using mTeSR and E8 or between with 1-d or 4-d RI for these static-suspension cultures (Figs. 1B and 2C). In summary, a combination of 10% (wt/vol) PNIPAAm-PEG, 4-d RI, defined E8, medium seeding density via single-cell or precluster seeding resulted in a high, 10.0-fold cell expansion in a single 4-d passage (Fig. 1 B and C). Final, fine-tuning of conditions revealed that 48 h RI was sufficient to support this expansion for precluster seeding, 4-d RI was required for single-cell seeding, and 8% (wt/vol) hydrogel performed as well as 10% (wt/vol) hydrogel (*SI Appendix*, Fig. S3).

We also assessed whether other, nonthermoreversible materials systems—including UV cross-linked hyarulonic acid (29), agarose (28), and alginate hydrogel (24)—could support high level hPSC expansion. We generated and used these materials as described previously, in conjunction with E8 and RI. For single-seeded iPS-MSCs, moderate expansion (∼2.8-fold) was seen only in alginate hydrogel with medium seeding density. A slightly higher, ∼5- or 6.5-fold expansion was achieved in agarose or alginate hydrogel for preclustered iPS-MSCs, respectively (*SI Appendix*, Fig. S4), although these numbers do not approach the levels of expansion observed with the thermoreversible material.

The multifactorial optimization thus resulted in an effective, completely defined system for hPSC culture, which was then characterized in greater detail. For both single-cell and cluster seeding, live/dead staining revealed very high viability within the hydrogel or spheroids (Fig. 3A). Also, 5-ethynyl-2′-deoxyuridine (EdU) staining showed uniform cell proliferation across spheroids, suggesting effective transport of nutrients, oxygen, and/or protein factors within the hydrogel and spheroids (Fig. 3B). Microscopy also revealed that single-seeded cells expanded and grew into spheroids with a narrow size distribution (e.g., 40–120 μm in diameter at day 5, Fig. 3C), whereas precluster seeding resulted in spheroids with larger sizes and broader distribution (50–300 μm in diameter at day 5, Fig. 3C). For both seeding methods, 10-, 20-, or 21-fold expansion, with final yields of ∼1, 2.0, or 2.1 × 10^7 cells per mL hydrogel, was achieved for hPSCs on day 4, 5, or 6 of the culture, respectively (Fig. 3D). Furthermore, immunostaining showed 95% of cells expressed pluripotency markers octamer-binding transcription factor 4 (Oct4) and Nanog, and alkaline phosphatase expression was both high
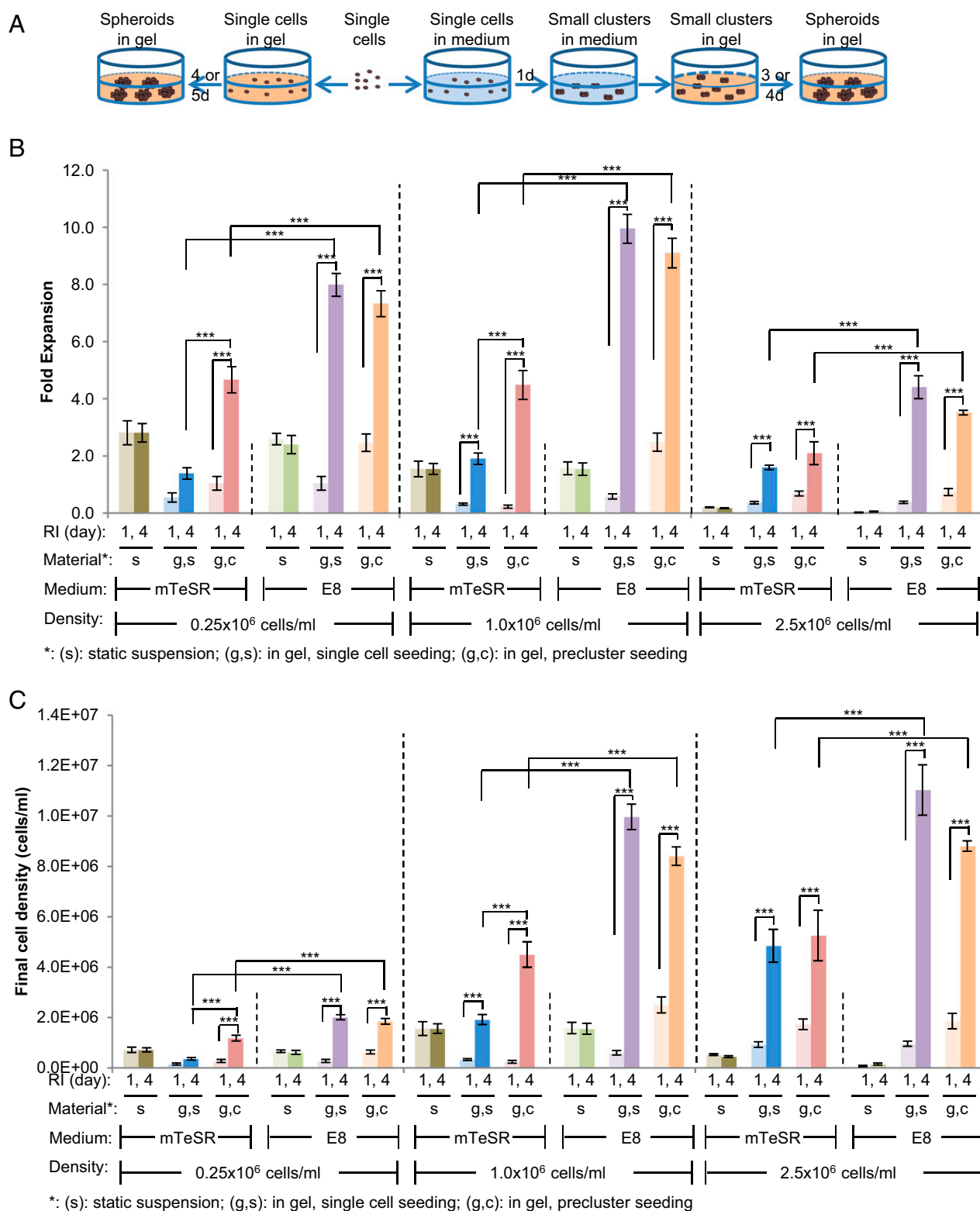
Fig. 1. A multifactorial experiment was designed to investigate the potential interactions between various system parameters. iPS-MSCs were cultured in static liquid medium without hydrogel (static suspension) or in 10% (wt/vol) PNIPAAm-PEG hydrogel via single-cell or precluster seeding for 4 d in mTeSR or E8 with 1- or 4-d RI at low, medium, or high seeding density (2.5×10^5, 1.0×10^6, or 2.5×10^6 cells/mL, respectively). (A) Schematic illustration of hPSC culture in 3D hydrogel. (B and C) Fold of expansion and final cell densities. The triple asterisk (***) indicates statistical significance at a level of $P < 0.001$.

and homogeneous across spheroids (Fig. 3 E–G). An additional 13-d culture was conducted to explore the sensitivity of cellular growth and pluripotency to spheroid size in this system. Single

iPS-MSCs were cultured in PNIPAAm-PEG hydrogel with E8 and RI for 13 d without passaging. An extremely low density (1.0×10^5 cells per mL) was used to provide sufficient space for cell
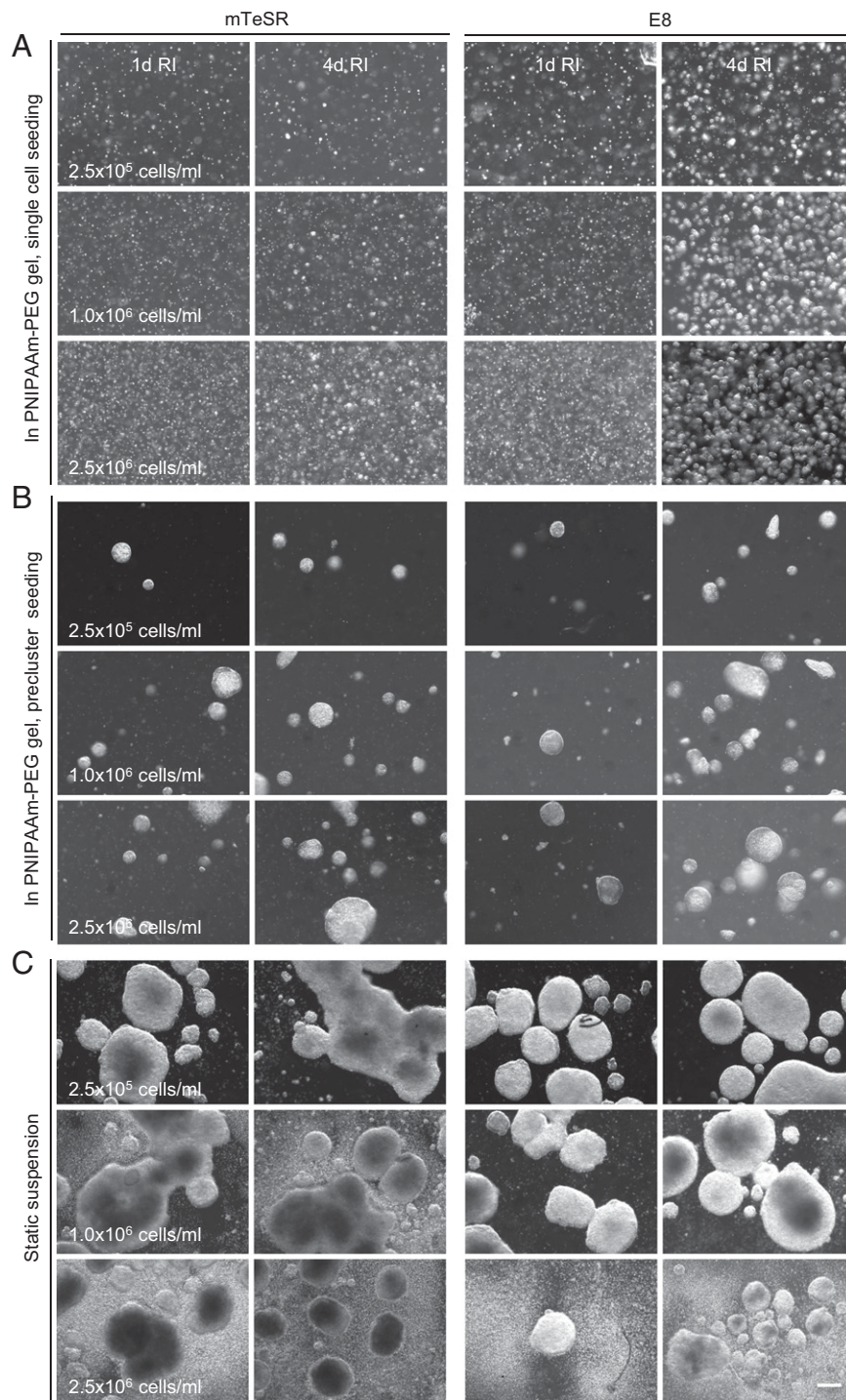
Fig. 2. Phase contrast images showing the cell morphologies for the factorial-designed experiment. iPS-MSCs were cultured in 10% PNIPAAm-PEG hydrogel via single cell (*A*) or precluster seeding (*B*) or in static liquid medium without hydrogel (static suspension) (*C*) for 4 days in mTeSR or E8 with 1d or 4d RI at low, medium or high seeding density (2.5×10^5, 1.0×10^6, or 2.5×10^6 cells per mL, respectively). (Scale bar: 250 μm.)

growth during the long 13-d culture. iPS-MSCs grew into spheroids with mean diameter of ∼350 μm, with the larger spheroids reached diameter up to ∼750 μm. Consistent cell growth and pluripotent marker expression were also seen in this size range (*SI Appendix,* Fig. S5). In summary, the culture system efficiently expanded hPSCs with high quality and density.

We next assessed the generality of this system for the long-term expansion of multiple hPSC lines (1, 33), which were con-

tinuously propagated for up to 60 passages or ∼280 d (with passaging every 4 or 5 d). During each of these passages, iPS-MSCs, iPS-Fib2 iPSCs, and H9 hESCs expanded ∼10- or 20-fold over 4 or 5 d, respectively, and H1 hESCs expanded 7-fold over 4 d, indicating some differences in growth rates among the lines (Fig. 4*A*). However, during this long-term culture with an accumulated expansion up to ∼10^{72}-fold, ∼95% of cells remained Oct4+ (Fig. 4*B*). Immunostaining again revealed uniform Nanog
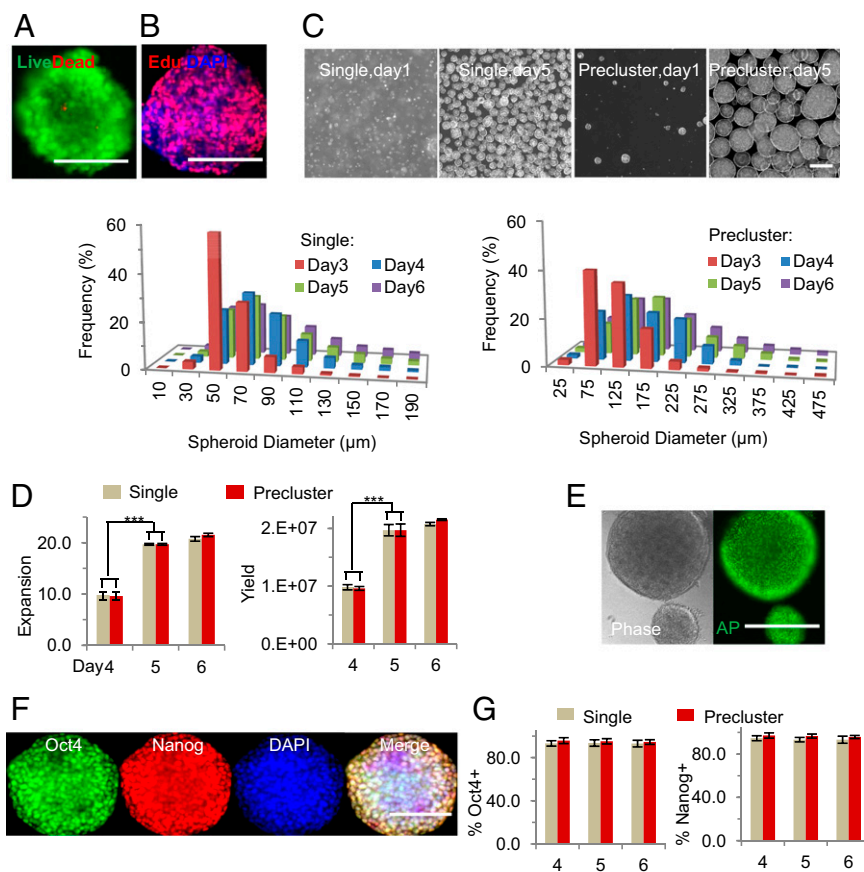
Fig. 3. A 6-d culture of hPSCs in 3D thermoreversible hydrogel. For both seeding methods, Live/Dead cell staining revealed a very high viability (*A*), and EdU pulse labeling demonstrated that cells proliferated uniformly across the spheroid (*B*). Spheroids on day 5 after precluster seeding are shown in *A* and *B*. (*C*) The morphology of spheroids on days 1 and 5 for both seeding methods and their size distribution are shown. The expansion fold and yield (cells per milliliter of hydrogel) on days 4, 5, and 6 were quantified (*D*). Immunostaining of spheroids, following precluster seeding and 3D hydrogel culture, shows that the majority of cells expressed the pluripotency markers alkaline phosphatase (*E*) as well as Oct4 and Nanog (*F*). (*G*) Approximately 95% of cells were Oct4+ or Nanog+. iPS-MSCs were used for *A*–*G*. The triple asterisk (***) indicates statistical significance at a level of $P < 0.001$. (Scale bar: 250 μm.)

and Oct4 expressions within spheroids (*SI Appendix*, Fig. S6). To our knowledge, this is the highest reported level of hPSC expansion in a culture system.

To assess whether cellular proliferation rates remained consistent over time, we reevaluated the growth kinetics of hPSCs after 10 passages in the gel. Notably, the expansion rate (~10-, 20-, or 21-fold at days 4, 5, or 6, respectively) (*SI Appendix*, Fig. S7), pluripotency marker expression, and spheroid size distribution (*SI Appendix*, Fig. S7) were similar to those at passage 1 (Fig. 3).

To further establish maintenance of cell pluripotency, embryoid body (EB) differentiation in vitro and teratoma formation in vivo were conducted after long-term culture within the hydrogel. Each cell line (iPS-MSC, iPS-Fib2, H9, H1) could undergo differentiation into the three germ layers, with expression of endodermal (HNF3β), mesodermal (αSMA), and ectodermal (Nestin) markers (Fig. 5*A* and *SI Appendix*, Fig. S8). Additionally, each hPSC line formed teratomas after 6–12 wk in vivo, and neural rosettes and epidermis from ectoderm, cartilage and muscle from mesoderm, and gut-like structure from endoderm were observed (Fig. 5*B* and *SI Appendix*, Fig. S9). In addition, hPSCs remained karyotypically normal after long-term culture within the gel (Fig. 5*C* and *SI Appendix*, Fig. S10).

To further assess whether hydrogel culture maintained cell behavior in 2D, after every 40 d in 3D, a passage of the hPSCs was returned to standard 2D surfaces. Dissociated cells attached to surfaces coated with vitronectin and grew into compact colonies after 4 d (*SI Appendix*, Fig. S11 *A* and *B*), and these cells could

subsequently undergo long-term expansion on 2D and maintain high Oct4+ levels (*SI Appendix*, Fig. S12). hPSCs could then be returned to the 3D culture system for additional expansion, indicating that cells can be interchanged between 2D and this 3D system as needed. Finally, cell banking is important for downstream applications, and hESCs expanded within the 3D system could be cryopreserved as single cells (*SI Appendix*, Fig. S11C).

Because suspension cultures are favored for large-scale production, we also demonstrated the hydrogel could readily be extruded into fibers (~2 mm in diameter) with encapsulated cells. Suspension of these fibers in 3D liquid culture resulted in ~19.5-fold expansion within 5 d for both single-cell and cell cluster seeding (*SI Appendix*, Fig. S13), yielding sufficiently high densities of encapsulated cell mass that the hydrogel fibers were opaque (*SI Appendix*, Fig. S13B). The pluripotency marker expression and spheroid size distribution (*SI Appendix*, Fig. S13 *C and D*) were indistinguishable from cells grown in hydrogels cast within a culture well (Fig. 3).

Biomedical applications for hPSCs entail differentiation into specific lineages, and we thus investigated whether cells after long-term culture in this system could then be directed into ectodermal, endodermal, or mesodermal lineages within the 3D material (Fig. 6). First, after a 4-d expansion in E8 medium and 9-d differentiation in neural induction medium with small molecule SMAD inhibitors in the 3D hydrogel (10), ~80% of H9-derived cells became positive for the neural progenitor markers Nestin and Pax6 (Fig. 6*A*). In a parallel culture, a 4-d
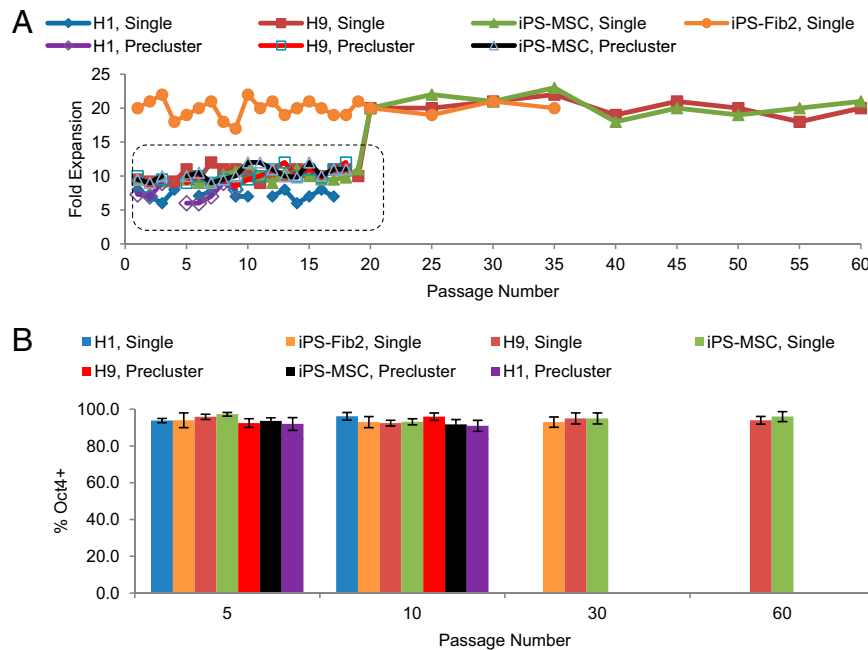
Fig. 4. Long-term, progressive expansion of hPSCs in the 3D hydrogel system. (*A*) The expansion rates of iPS-MSCs, iPS-Fib2s, H9s, and H1s at each passage (4 or 5 d) using single-cell or precluster seeding are shown. Passages with 4 d are indicated (dotted line). (*B*) Oct4 levels remained high during the long-term culture.

expansion in E8 medium and 5-d differentiation in endoderm induction medium (4) in the 3D hydrogel resulted in ~95% of H9 or iPS-MSC–derived cells being positive for the endoderm progenitor markers forkhead box protein A2 (FOXA2) and SOX17 (Fig. 6*B*). Finally, a 4-d expansion in E8 medium and 9-d differentiation in cardiomyocyte induction medium (34) within the 3D hydrogel yielded beating spheroids 2 d after transfer to a fibronectin-coated plate (Movie S1).

Several clinical trials have demonstrated that fetal ventral midbrain tissue implants can alleviate motor symptoms in Parkinson patients under certain circumstances, although this approach is challenged by tissue supply and other considerations (35, 36). In recent important work, Kriks et al. (10) and Kirkeby et al. (37) developed approaches for differentiating hPSCs into DA progenitors or neurons that could functionally integrate into the brains of mouse, rat, and nonhuman primate models of PD. We investigated whether the differentiation protocols—which included both defined (Noggin, Shh, FGF8, TGFβ3) and undefined protein components—could be adapted to 3D culture under defined conditions. DA induction of H9 spheroids (40–120 μm) within the hydrogel was initiated via dual SMAD inhibition, Shh, and a GSK3β inhibitor to activate Wnt signaling (Fig. 7*A*). On day 11, 81% of cells within the spheroids (~100–300 μm) were positive for the ventral midbrain DA progenitor markers FOXA2 and LMX1a (Fig. 7 *B–D*). These matched levels obtained in 2D; however, cells in 3D expanded ~80-fold over 15 d, resulting in 8×10^7 cells per mL of hydrogel, compared with only an approximately ninefold expansion on 2D surface (Fig. 7*D*). Finally, these DA progenitors could subsequently be cultured on 2D surfaces as described (37) for differentiation into mature TH+ DA neurons (Fig. 7*E*).

Discussion

Large numbers of hPSCs, or their differentiated progeny, are needed for many biomedical applications (9). For large-scale expansion, currently hPSCs from a cell bank are expanded into large numbers through progressive proliferation followed by directed differentiation into progenitors or mature cells. Efficient,

scalable, and GMP-compliant culture systems are required for such processes (9). hPSC culture has made considerable progress, but current systems achieve only moderate expansion, yield, and quality (9) (*SI Appendix*, Table S1). The most effective system reported to date enabled approximately threefold to fourfold expansion of hESCs per passage in mTeSR medium containing 1% BSA, for a final yield of $<1 \times 10^6$ cells per mL (18) (*SI Appendix*, Table S1). We have developed a 3D culture system—which combines a synthetic thermoreversible hydrogel and defined medium with an optimized protocol involving single-cell passaging—for simple, defined, scalable, and GMP-compliant hESC and hiPSC expansion (Figs. 1–5) and differentiation (Figs. 6 and 7) with high yield. Long-term culture (>280 d) with high expansion rate (20-fold over 5 d, or 6.4×10^7-fold over 1 mo, and 10^{72}-fold over 280 d), volumetric cell yield (2×10^7 cells per mL of hydrogel), and quality (~95% Oct4+) were achieved (Figs. 3 and 4). Additionally, the hPSCs were able to differentiate into all of the three germ layers after long-term culture in the 3D system (Fig. 5 and *SI Appendix*, Figs. S8 and S9). Finally, the 3D system also supported directed differentiation into neural progenitors, endoderm progenitors (Fig. 6), beating cardiomyocytes (Movie S1), or midbrain dopaminergic progenitors (Fig. 7) by simply replacing the expansion medium with the differentiation medium. This versatile system thus combines many advantageous and important features.

The survival and proliferation of hESCs and hiPSCs—which both exhibit characteristics typical of epiblast-like pluripotent stem cells (14)—depend on multiple extracellular cues. These include soluble protein growth factors [e.g., FGF2, TGF-β, and autocrine/paracrine cues (15)] that signal via a number of pathways to support cell survival and pluripotency factors [e.g., Nanog, Oct4, Sox2 (38–40)]. In addition, hPSCs engage in cell–matrix interactions (31), and cell–cell contacts via cadherins are particularly important for survival and pluripotency maintenance. Disruption of such cell–cell contacts leads to Abr-dependent activation of RhoA (and inactivation of Rac1), ROCK activation, and downstream actomyosin hyperactivation and apoptosis (14, 32). Other environ-
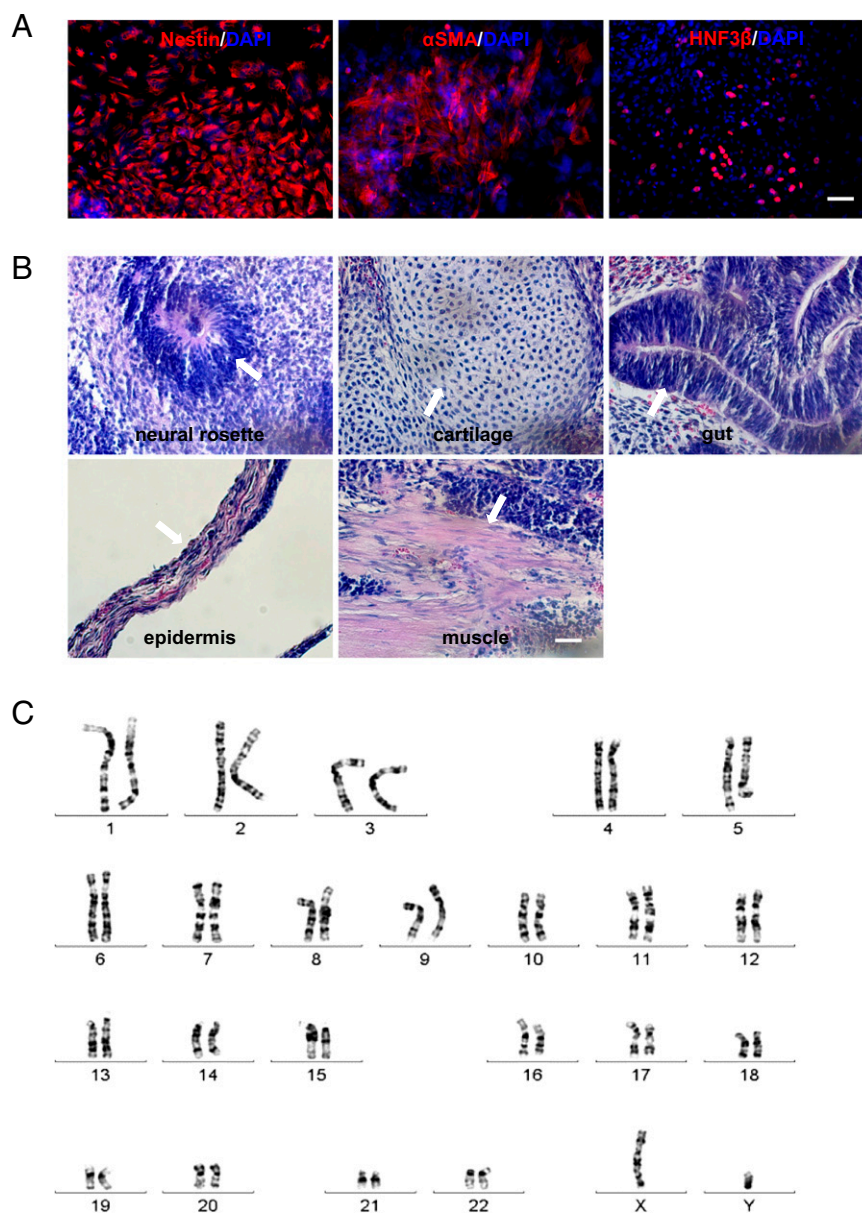
Fig. 5. hPSCs retained pluripotency and normal karyotype after long-term culture in the 3D hydrogel system. (*A*) EB differentiation in vitro. iPS-MSCs were expanded in the 3D hydrogel for 35 passages via single-cell seeding before EB differentiation. Immunostaining for the three germ layers (ectoderm: Nestin; mesoderm: αSMA; and endoderm: HNF3β) are shown. (*B*) Teratoma formation in vivo. iPS-MSCs expanded in 3D hydrogels for 35 passages via single-cell seeding were injected into mice s.c., and teratomas formed after 6–12 wk. Structures from all three germ layers (arrows) were identified, including ectoderm: neural rosette and epidermis; mesoderm: cartilage and muscle; and endoderm: gut-like-structure. (*C*) iPS-MSCs cultured in the 3D hydrogel for 35 passages via single-cell seeding retained normal karyotypes. (Scale bars: *A*, 100 μm; *B*, 50 μm.)

mental stress, such as mechanical forces (9, 41) or apparently redox conditions (3), can also adversely affect cell function.

Through a combination of rational and empirical investigation, this culture system based on a thermoresponsive material apparently addresses a number of these needs. Importantly, multifactorial investigation indicated that the system's properties may result from a combination of the synthetic PNIPAAm-PEG matrix, defined medium, and optimized protocol, as any of these elements alone yielded suboptimal outcomes (Figs. 1 and 2, and *SI Appendix*, Figs. S1–S5 and S13–S15). The culture medium provides key soluble cues (3), and the material may conceivably concentrate autocrine/paracrine factors near cells (15). RI ameliorates dissociation-induced apoptosis that otherwise occurs via cytoskeletal-associated pathways (14, 31, 32), and future inves-

tigation may elucidate whether this mechanically soft (*SI Appendix*, Fig. S14) thermoresponsive material may more favorably interface with these mechanosensitive pathways relative to other materials (14). The material also protects cells from shear-induced stress, yet this readily deformable hydrogel may more favorably allow single-cell division and subsequent cluster growth relative to chemically cross-linked hyaluronic acid, ionically associated alginate, or stiff agarose hydrogels. Finally, E8 unlike mTeSR lacks β-mercaptoethanol, an apparent stressor of hESCs, particularly in suboptimal culture environments (*SI Appendix*, Fig. S15). A combination of factors thus interacts to provide a permissive 3D system that supports hPSC biology, and future investigations may elucidate the mechanistic contributions of both biochemical and mechanical features of this microenvironment.
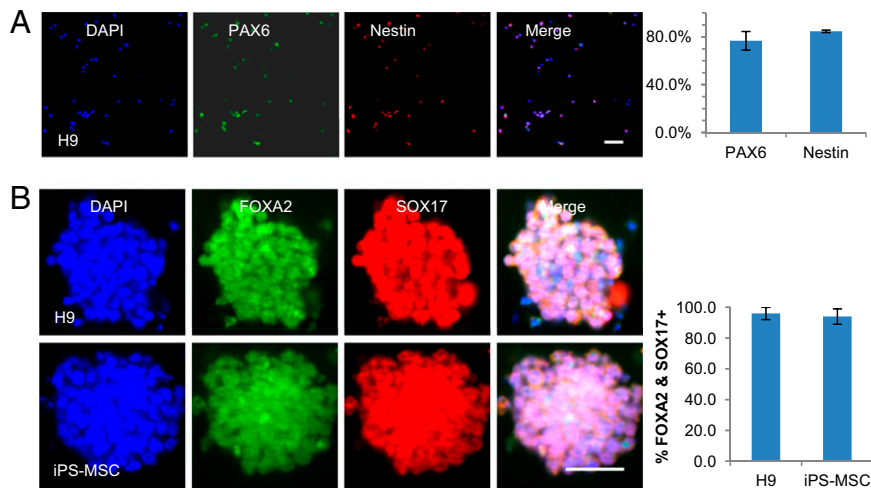
Fig. 6. Neural and endodermal induction in the 3D hydrogel. hPSCs that had been cultured in the 3D system for 20–30 passages were used for differentiation. (*A*) After 4 d of expansion and 9 d of dual SMAD inhibition, ~80% of differentiated H9s were positive for neuroectodermal markers Nestin or PAX6. The spheroids were dissociated into single cells before staining. (*B*) After 4 d of expansion and 3 d of endodermal induction, ~95% of differentiated H9s or iPS-MSCs were positive for endodermal progenitor markers FOXA2 and SOX17. (Scale bar: 100 µm.)

The system can also be adapted to multiple scales—from the laboratory toward the clinic—to support research in cell replacement therapies, artificial tissues and organs, and/or high-throughput drug screening/toxicity screening with hPSCs. For instance, ~50 mL of hydrogel would be sufficient to produce 10^9 cells for preclinical animal studies, and a bioreactor with ~5 L of hydrogel could yield $>10^{11}$ cells for clinical studies. The ability to move a single culture system through multiple scales may aid clinical development.

Advances in developmental and stem cell biology have enabled the development of approaches to effectively differentiate hPSCs into numerous additional cell types, such as neural crest
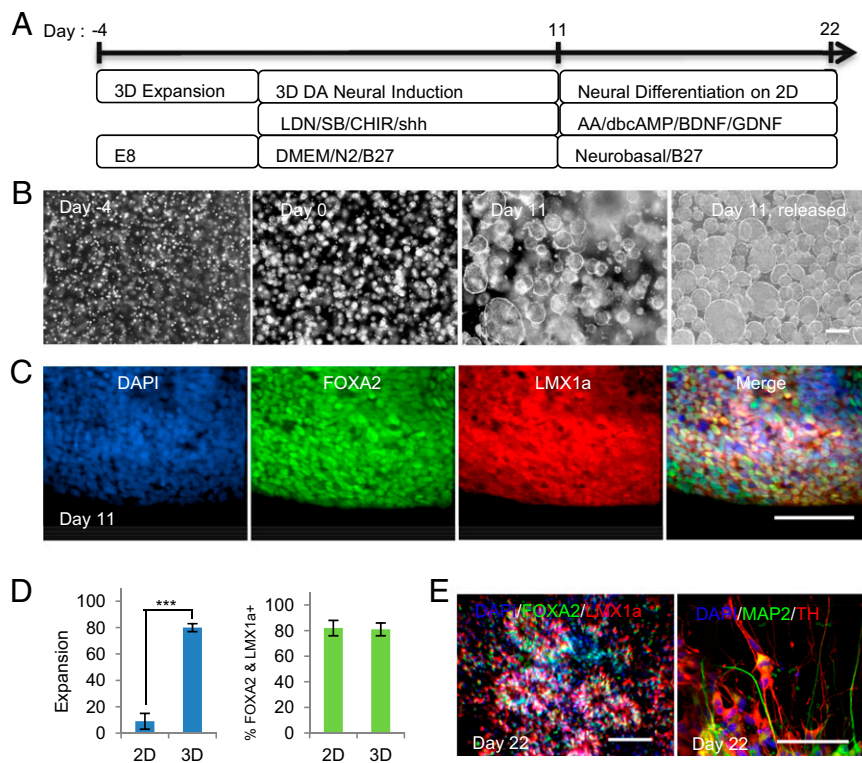

Fig. 7. Scalable production of dopaminergic (DA) neuron progenitors in the 3D culture system. (*A*) Protocol used for generating DA progenitors in 3D. (*B*) Phase images showing spheroid morphologies during the 15-d production process, as well as spheroids released from the hydrogel on day 11. (*C*) Immunostaining on day 11 for the midbrain DA progenitor makers FOXA2 and LMX1a. (*D*) The fold of expansion and percentage of FOXA2 and LMX1a double-positive cells on day 11 in the 3D hydrogel system or on the conventional 2D surface. (*E*) The day 11 DA progenitors produced in the 3D system matured into TH+ DA neurons after 11 additional days in culture on 2D laminin surfaces. hPSCs cultured in the 3D system for 20–30 passages were used for these differentiation. The triple asterisk (***) indicates statistical significance at a level of *P* < 0.001. (Scale bars: *B*, 250 µm; *C* and *E*, 100 µm.)

cells (42), motor neurons (43), oligodendrocyte progenitors (44, 45), pancreatic progenitors (4, 46), hepatocyte-like cells (47), retinal cells (48), and others (49, 50). Several of these processes have even proceeded to clinical trials (51). Future work can explore integrating these advances into this defined 3D hydrogel culture system to aid efficient, economical, and reproducible cell production for multiple future applications.

Methods

Maintaining hPSCs on 2D Surface. Human ESC lines H1 and H9 were obtained from WiCell Research Institute. iPS-MSC (33) (derived from human MSCs) and iPS-Fib2 (33) (derived from human dermal fibroblasts) were gift from George Q. Daley (Children's Hospital Boston, Boston). hPSCs were cultured on six-well plate coated with vitronectin (Invitrogen) in E8 medium (Invitrogen). Cells were passaged every 4 d with 0.5 mM EDTA (Invitrogen). To replate hPSCs on 2D surfaces following expansion within the 3D hydrogel, hPSC spheroids were dissociated with Accutase (Life Technologies) at 37 °C for 10 min, and cultured on six-well plate coated with vitronectin in E8 medium (supplied with 10 μM ROCK inhibitor, Y-27632, Selleckchem, for the first 24 h).

Expanding hPSCs in 3D Hydrogel. To transfer the culture from 2D to 3D, hPSCs on Matrigel or vitronectin-coated tissue culture plates were incubated with Accutase at 37 °C for 5 min and dissociated into single cells. For the single-cell seeding method, dissociated cells were mixed with PNIPAAm-PEG (Cosmo Bio) solution dissolved in E8 medium at 4 °C and cast on tissue culture plate, then incubated at 37 °C for 15 min to form hydrogels before adding warm E8 medium containing 10 μM ROCK inhibitor. For the precluster seeding method, dissociated cells were cultured in suspension overnight in low adhesion plates to form small clusters that were subsequently encapsulated into the 3D hydrogel as mentioned above.

To passage hPSCs within 3D hydrogel, ice-cold PBS was added to the 3D culture at day 4 or 5 to dissolve the gel. Spheroids were collected by centrifuging at 200 × g for 3 min, incubated with Accutase at 37 °C for 10 min, and dissociated into single cells for reencapsulation as mentioned above. The NucleoCounter NC-200 (Chemometec) was used to count cell numbers. To prepare hydrogel fibers, a 4 °C PNIPAAm-PEG solution containing cells was extruded into room temperature E8 medium through a 2-mm-diameter tube. The resulting hydrogel fibers were cultured in suspension in E8 medium at 37 °C. Medium was changed daily for all cultures. To measure spheroid sizes, hPSCs were released from the hydrogel, and phase images were taken. The diameters of >2,000 spheroids were quantified with MetaXpress software (Molecular Devices). The frequency of spheroids within a diameter range was calculated with the Excel Histogram Plug-in. Expanded cells were cryopreserved as single cells in E8 medium with 10% (vol/vol) DMSO and 10 μM ROCK inhibitor in liquid N$_2$.

Staining and Imaging. Cells cultured on 2D surfaces were fixed with 4% (wt/vol) paraformaldehyde (PFA) at room temperature for 15 min, permeabilized with 0.25% Triton X-100 for 15 min, and blocked with 5% (vol/vol) goat serum for 1 h before incubating with primary antibodies at room temperature for 2 h. After extensive washing, secondary antibodies in 2% (wt/vol) BSA were added and incubated for another 1 h. Cells were washed with PBS for three times before imaging.

To assess the pluripotency marker expression of cells expanded in 3D hydrogels, hPSCs were dissociated into single cells with Accutase and stained in suspension. Cells were then placed in 96-well plates and analyzed with an ImageXpress (Molecular Devices). The percentage of Oct4+ or Nanog+ nuclei was quantified with MetaXpress software (Molecular Devices). This process was used to quantify the PAX6+ and Nestin+ cells after neural induction as well.

To stain spheroids, hPSCs were fixed with 4% (wt/vol) PFA at room temperature for 30 min, and then incubated with PBS plus 0.25% Triton X-100 plus 5% (vol/vol) goat serum plus primary antibodies at 4 °C for 48 h. After extensive washing, secondary antibodies in 2% (wt/vol) BSA were added and incubated at 4 °C for 4 h. Cells were washed with PBS for three times before imaging. Staining without primary antibodies was used as controls for all of the immunostainings.

LIVE/DEAD Cell Viability staining (Invitrogen) was used to assess live and dead cells, the Click-iT EdU Alexa Fluor 594 Imaging Kit (Invitrogen) was used to label proliferating cells, and an Alkaline Phosphatase Live Stain (Invitrogen) was used to image alkaline phosphatase.

EB Differentiation. hPSCs were suspended in DMEM plus 20% (vol/vol) FBS plus 10 μM β-mercaptoethanol in low adhesion plates for 6 d. The EBs were then transferred onto plates coated with 0.1% gelatin and cultured in the same medium for another 6 d, followed by fixation and staining as above.

Teratoma Formation in Vivo. All animal protocols were approved by the Animal Care and Use Committee of the University of California, Berkeley. A total of 3×10^6 hPSCs was suspended in 25 μL of PBS plus 25 μL of Matrigel (BD Biosciences) and injected s.c. at the back of the neck of the SCID Beige mice (Charles River Laboratory), and teratomas were harvested when sizes reached 2 cm. The tissue was then fixed with 4% (wt/vol) PFA for 48 h, dehydrated with 70%, 95%, and 100% (vol/vol) ethanol sequentially, and defatted with xylene for 2 h before embedding in paraffin. The 10-μm-thick sections were cut and stained with hematoxylin and eosin.

Karyotype. Kyarotyping was performed by Oakland Children's Hospital Cytogenetics Laboratory.

Neural Induction (52). Following expansion, hPSCs were cultured in knockout serum replacement (KSR) medium with 10 μM SB431542 (Selleckchem) and 100 nM LDN193189 (Selleckchem) for 5 d. Starting at day 5, the KSR medium was gradually replaced by the N2 medium, and cells were harvested at day 9. KSR medium was as follows: DMEM plus 15% (vol/vol) KSR plus 2 mM glutamine plus 10 μM β-mercaptoethanol. N2 medium was as follows: Neurobasal plus N2 plus B27 (without retinoic acid) plus 2 mM L-glutamine.

Endodermal Induction (4). Following expansion, hPSCs were cultured in RPMI 1640 (Sigma) plus 0.2% FBS plus 100 ng/mL Activin-A (Peprotech) plus 20 ng/mL Wnt3a (R&D) for 1 d and in RPMI 1640 plus 0.5% FBS plus 100 ng/mL Activin-A for 2 more days before being fixed and immunostained.

Cardiomyocyte Differentiation (34). Following expansion, hPSCs were cultured in RPMI 1640 plus B27 without insulin between day 0 and 7, and in RPMI 1640 plus B27 after. The following small molecules were added: 12 μM CHIR99021 (Selleckchem) for days 0–1; 5 μM IWP-2 Inhibitor (Selleckchem) for days 3–5. Spheroids were released on day 9 to fibronectin-coated plate. Beating cardiomyocytes were filmed on day 11.

Differentiating hPSCs into Dopaminergic Neuronal Progenitors. hPSCs were cultured in 50% DMEM/F12 plus 50% (vol/vol) Neurobasal medium (with 1:100 N2 and 1:50 B27) for 11 d following expansion (37). The following proteins and small molecules were added: 10 μM SB431542; 200 ng/mL Noggin (R&D) or (100 nM LDN193189); 0.7 μM CHIR99021 and 200 ng/mL SHH C25II. Cells were harvested at day 11.

Statistical Analysis. Statistical analyses were done using the statistical package Instat (GraphPad Software). For multiple comparisons, the means of triplicate samples were compared using the Tukey multiple-comparisons analysis with the α level indicated in the figure legend.

Antibodies. Oct4 (Santa Cruz Biotechnology; 1:100), Nanog (Santa Cruz Biotechnology; 1:100), Nestin (Millipore; 1:200), αSMA (Abcam; 1:200), FOXA2/HNF3β (Santa Cruz Biotechnology; 1:200), PAX6 (Covance; 1:200), LMX1a (Millipore; 1:1,000), MAP2 (BD Biosciences; 1:1,000), TH (Pel-Freez; 1:1,000), and SOX17 (R&D; 1:500).

1. Thomson JA, et al. (1998) Embryonic stem cell lines derived from human blastocysts. *Science* 282(5391):1145–1147.
2. Takahashi K, et al. (2007) Induction of pluripotent stem cells from adult human fibroblasts by defined factors. *Cell* 131(5):861–872.
3. Chen G, et al. (2011) Chemically defined conditions for human iPSC derivation and culture. *Nat Methods* 8(5):424–429.
4. Schulz TC, et al. (2012) A scalable system for production of functional pancreatic progenitors from human embryonic stem cells. *PLoS One* 7(5):e37004.
5. Lindvall O, Kokaia Z, Martinez-Serrano A (2004) Stem cell therapy for human neurodegenerative disorders-how to make it work. *Nat Med* 10(Suppl):S42–S50.
6. Badylak SF, Taylor D, Uygun K (2011) Whole-organ tissue engineering: Decellularization and recellularization of three-dimensional matrix scaffolds. *Annu Rev Biomed Eng* 13:27–53.
7. McNeish J (2004) Embryonic stem cells in drug discovery. *Nat Rev Drug Discov* 3(1):70–80.
8. Desbordes SC, Studer L (2013) Adapting human pluripotent stem cells to high-throughput and high-content screening. *Nat Protoc* 8(1):111–130.

9. Serra M, Brito C, Correia C, Alves PM (2012) Process engineering of human pluripotent stem cells for clinical application. *Trends Biotechnol* 30(6):350–359.

10. Kriks S, et al. (2011) Dopamine neurons derived from human ES cells efficiently engraft in animal models of Parkinson's disease. *Nature* 480(7378):547–551.

11. Laflamme MA, Murry CE (2005) Regenerating the heart. *Nat Biotechnol* 23(7): 845–856.

12. Roger VL, et al. (2012) Heart disease and stroke statistics—2012 update: A report from the American Heart Association. *Circulation* 125(1):e2–e220.

13. Zang R, Li D, Tang I, Wang J, Yang S (2012) Cell-based assays in high-throughput screening for drug discovery. *Int J Biotechnol Wellness Ind* 1:31–51.

14. Ohgushi M, Sasai Y (2011) Lonely death dance of human pluripotent stem cells: ROCKing between metastable cell states. *Trends Cell Biol* 21(5):274–282.

15. Peerani R, et al. (2007) Niche-mediated control of human embryonic stem cell self-renewal and differentiation. *EMBO J* 26(22):4744–4755.

16. Villa-Diaz LG, Ross AM, Lahann J, Krebsbach PH (2013) Concise review: The evolution of human pluripotent stem cell culture: From feeder cells to synthetic coatings. *Stem Cells* 31(1):1–7.

17. McDevitt TC, Palecek SP (2008) Innovation in the culture and derivation of pluripotent human stem cells. *Curr Opin Biotechnol* 19(5):527–533.

18. Chen VC, et al. (2012) Scalable GMP compliant suspension culture system for human ES cells. *Stem Cell Res (Amst)* 8(3):388–402.

19. Steiner D, et al. (2010) Derivation, propagation and controlled differentiation of human embryonic stem cells in suspension. *Nat Biotechnol* 28(4):361–364.

20. Amit M, et al. (2011) Dynamic suspension culture for scalable expansion of undifferentiated human pluripotent stem cells. *Nat Protoc* 6(5):572–579.

21. Zweigerdt R, Olmer R, Singh H, Haverich A, Martin U (2011) Scalable expansion of human pluripotent stem cells in suspension culture. *Nat Protoc* 6(5):689–700.

22. Nie Y, Bergendahl V, Hei DJ, Jones JMPS, Palecek SP (2009) Scalable culture and cryopreservation of human embryonic stem cells on microcarriers. *Biotechnol Prog* 25(1):20–31.

23. Chen AK, Chen X, Choo AB, Reuveny S, Oh SK (2011) Critical microcarrier properties affecting the expansion of undifferentiated human embryonic stem cells. *Stem Cell Res (Amst)* 7(2):97–111.

24. Serra M, et al. (2011) Microencapsulation technology: A powerful tool for integrating expansion and cryopreservation of human embryonic stem cells. *PLoS One* 6(8): e23212.

25. Unger C, Skottman H, Blomberg P, Dilber MS, Hovatta O (2008) Good manufacturing practice and clinical-grade human embryonic stem cell lines. *Hum Mol Genet* 17(R1): R48–R53.

26. Medina RJ, Kataoka K, Takaishi M, Miyazaki M, Huh NH (2006) Isolation of epithelial stem cells from dermis by a three-dimensional culture system. *J Cell Biochem* 98(1): 174–184.

27. Chayosumrit M, Tuch B, Sidhu K (2010) Alginate microcapsule for propagation and directed differentiation of hESCs to definitive endoderm. *Biomaterials* 31(3):505–514.

28. Stenberg J, et al. (2011) Sustained embryoid body formation and culture in a non-laborious three dimensional culture system for human embryonic stem cells. *Cytotechnology* 63(3):227–237.

29. Gerecht S, et al. (2007) Hyaluronic acid hydrogel for controlled self-renewal and differentiation of human embryonic stem cells. *Proc Natl Acad Sci USA* 104(27): 11298–11303.

30. Watanabe K, et al. (2007) A ROCK inhibitor permits survival of dissociated human embryonic stem cells. *Nat Biotechnol* 25(6):681–686.

31. Xu Y, et al. (2010) Revealing a core signaling regulatory mechanism for pluripotent stem cell survival and self-renewal by small molecules. *Proc Natl Acad Sci USA* 107(18): 8129–8134.

32. Ohgushi M, et al. (2010) Molecular pathway and cell state responsible for dissociation-induced apoptosis in human pluripotent stem cells. *Cell Stem Cell* 7(2):225–239.

33. Park I-H, et al. (2008) Reprogramming of human somatic cells to pluripotency with defined factors. *Nature* 451(7175):141–146.

34. Lian X, et al. (2012) Robust cardiomyocyte differentiation from human pluripotent stem cells via temporal modulation of canonical Wnt signaling. *Proc Natl Acad Sci USA* 109(27):E1848–E1857.

35. Lindvall O (2013) Developing dopaminergic cell therapy for Parkinson's disease—give up or move forward? *Mov Disord* 28(3):268–273.

36. Mendez I, et al. (2008) Dopamine neurons implanted into people with Parkinson's disease survive without pathology for 14 years. *Nat Med* 14(5):507–509.

37. Kirkeby A, et al. (2012) Generation of regionally specified neural progenitors and functional neurons from human embryonic stem cells under defined conditions. *Cell Rep* 1(6):703–714.

38. Xu R-H, et al. (2008) NANOG is a direct target of TGFbeta/activin-mediated SMAD signaling in human ESCs. *Cell Stem Cell* 3(2):196–206.

39. Vallier L, Alexander M, Pedersen RA (2005) Activin/Nodal and FGF pathways cooperate to maintain pluripotency of human embryonic stem cells. *J Cell Sci* 118(Pt 19): 4495–4509.

40. James D, Levine AJ, Besser D, Hemmati-Brivanlou A (2005) TGFbeta/activin/nodal signaling is necessary for the maintenance of pluripotency in human embryonic stem cells. *Development* 132(6):1273–1282.

41. Hsieh MH, Nguyen HT (2005) Molecular mechanism of apoptosis induced by mechanical forces. *Int Rev Cytol* 245:45–90.

42. Lee G, Chambers SM, Tomishima MJ, Studer L (2010) Derivation of neural crest cells from human pluripotent stem cells. *Nat Protoc* 5(4):688–701.

43. Hu B-Y, Zhang S-C (2009) Differentiation of spinal motor neurons from pluripotent human stem cells. *Nat Protoc* 4(9):1295–1304.

44. Keirstead HS, et al. (2005) Human embryonic stem cell-derived oligodendrocyte progenitor cell transplants remyelinate and restore locomotion after spinal cord injury. *J Neurosci* 25(19):4694–4705.

45. Sharp J, Frame J, Siegenthaler M, Nistor G, Keirstead HS (2010) Human embryonic stem cell-derived oligodendrocyte progenitor cell transplants improve recovery after cervical spinal cord injury. *Stem Cells* 28(1):152–163.

46. Kroon E, et al. (2008) Pancreatic endoderm derived from human embryonic stem cells generates glucose-responsive insulin-secreting cells in vivo. *Nat Biotechnol* 26(4): 443–452.

47. Duan Y, et al. (2010) Differentiation and characterization of metabolically functioning hepatocytes from human embryonic stem cells. *Stem Cells* 28(4):674–686.

48. Osakada F, Ikeda H, Sasai Y, Takahashi M (2009) Stepwise differentiation of pluripotent stem cells into retinal cells. *Nat Protoc* 4(6):811–824.

49. Cheung C, Sinha S (2011) Human embryonic stem cell-derived vascular smooth muscle cells in therapeutic neovascularisation. *J Mol Cell Cardiol* 51(5):651–664.

50. Descamps B, Emanueli C (2012) Vascular differentiation from embryonic stem cells: Novel technologies and therapeutic promises. *Vascul Pharmacol* 56(5-6):267–279.

51. Trounson A, Thakar RG, Lomax G, Gibbons D (2011) Clinical trials for stem cell therapies. *BMC Med* 9:52.

52. Chambers SM, et al. (2009) Highly efficient neural conversion of human ES and iPS cells by dual inhibition of SMAD signaling. *Nat Biotechnol* 27(3):275–280.